Complete breakdown of the Debye model of rotational relaxation near the isotropic-nematic phase boundary: Effects of intermolecular correlations in orientational dynamics

Prasanth P. Jose, Dwaipayan Chakrabarti, and Biman Bagchi*

Solid State and Structural Chemistry Unit, Indian Institute of Science, Bangalore 560012, Karnataka, India

The Debye-Stokes-Einstein (DSE) model of rotational diffusion predicts that the orientational correlation times τ_l vary as $[l(l+1)]^{-1}$, where l is the rank of the orientational time correlation function (given in terms of the Legendre polynomial of rank l). One often finds significant deviation from this prediction, in either direction. In supercooled molecular liquids where the ratio τ_1/τ_2 falls considerably below 3 (the Debye limit), one usually invokes a jump diffusion model to explain the approach of the ratio τ_1/τ_2 to unity. Here we show in a computer simulation study of a standard model system for thermotropic liquid crystals that this ratio becomes much less than unity as the isotropic-nematic phase boundary is approached from the isotropic side. Simultaneously, the ratio τ_2/η, η being the shear viscosity of the liquid, becomes much larger than the hydrodynamic value near the *I-N* transition. We also analyze the breakdown of the Debye model of rotational diffusion in ratios of higher order orientational correlation times. We show that the breakdown of the DSE model is due to the growth of orientational pair correlation and provide a mode coupling theory analysis to explain the results.

PACS number(s): 61.30.−v, 66.10.Cb

I. INTRODUCTION

The rotational diffusion model of Debye [1,2] was proposed originally to explain dielectric relaxation of polar molecules. For large Brownian particles reorienting in a liquid in small steps, the Debye model predicts an exponential decay for the lth rank single-particle orientational time correlation function (OTCF) $C_l^s(t)$

$$C_l^s(t) = \exp(-t/\tau_l), \qquad (1)$$

and gives for the corresponding orientational correlation time τ_l

$$\tau_l = \frac{1}{l(l+1)D_r}, \qquad (2)$$

where D_r is the rotational diffusion coefficient. The latter is predicted to be coupled with the shear viscosity η at any temperature T by the Debye-Stokes-Einstein (DSE) relationship that relies upon hydrodynamic assumptions

$$D_r = \frac{k_B T}{V_H \eta}. \qquad (3)$$

The hydrodynamic volume V_H is related to the molecular volume v through a factor that depends on the shape of the reorienting particle and the boundary conditions. For example, $V_H = 6v$ for a sphere with stick boundary conditions. In spite of the involvement of hydrodynamic assumptions, the DSE relationship is known to be effective down to the molecular length scales for low-viscosity liquids. The DSE relationship has been found to work well when tested in experiments and simulations for dependence on shape, size,

and boundary conditions in low-viscosity simple as well as complex liquids [3–5].

It follows that the Debye model of rotational diffusion predicts the $[l(l+1)]^{-1}$ dependence for τ_l, and specifically the ratio of the first and second-rank orientational correlation times, τ_1/τ_2, to be equal to 3. A significant deviation from this ratio is taken to be the signature of the breakdown of the Debye model [6]. In particular, the ratio is known to approach unity at temperatures close to the glass transition temperature T_g in supercooled liquids [7,8]. One often relates the emergence of hopping involving large angular jumps to this breakdown of Debye diffusion model, which requires small angle Brownian rotational motion for its validity [8]. The basic idea is that a large jump leads to the decay of $C_l^s(t)$ of all ranks l at the same time, so that all of them have similar correlation times corresponding to the average waiting time for this large jump to occur.

The DSE relationship was found to conform well to the experimental data from NMR studies [9,10] and time-resolved optical spectroscopy using photobleaching techniques [11,12] even in highly viscous supercooled liquids close to T_g. This is often discussed in the context of translation-rotation decoupling in supercooled liquids and the relevant issues have drawn considerable attention [13–18]. However, a number of experimental and computational studies provided evidence for the failure of the DSE relationship at high viscosities in supercooled molecular liquids and glassy polymers [19–23]. An overestimation of the orientational correlation times by the DSE relationship was apparent from time resolved fluorescence and electron spin resonance (ESR) studies on tracer reorientation [23,24]. It is notable that an ESR study revealed jump motion for reorientation of the probe at the temperature regime where probe reorientation was found to get decoupled from the viscosity according to ESR studies [22,25].

The case of τ_1/τ_2 deserves particular attention because it is the oft-discussed one, both τ_1 and τ_2 being experimentally

*Electronic address: bbagchi@sscu.iisc.ernet.in

accessible [6–8]. However, the sensitivity of the respective OTCFs (and hence the corresponding orientational correlation times) to intermolecular interactions is different. When the rotating molecule has dipolar interactions with the surrounding molecules, one expects the first rank OTCF to be more affected than the second rank one. This is a manifestation of long-range intermolecular correlation which is reflected in the orientational pair correlation functions. Thus, if we consider dipolar spheres (such as Stockmayer liquid), we should expect the ratio τ_1/τ_2 to be larger than three [26]. On the other hand, if the intermolecular interaction has up-down symmetry (as is the case with ellipsoids of revolution), the reverse could be true.

One ideal candidate to test the above argument regarding the role of equilibrium pair correlations is a system of model mesogens undergoing the isotropic-nematic (*I-N*) phase transition. The isotropic phase is both positionally and orientationally disordered while the nematic phase is still positionally disordered but orientationally ordered. The orientational order parameter, defined by $S=\langle P_2[\cos(\theta)]\rangle$, θ being the angle between the molecular axis getting ordered with the director, serves to characterize the *I-N* transition. In the isotropic phase, $S=0$ for infinitely large systems (for *N*-particle system, $S\simeq 1/\sqrt{N}$) while it is nonzero (around 0.5) in the nematic phase. The important point is that orientational correlation undergoes rapid increase as the *I-N* phase boundary is approached from the isotropic side. This large growth in correlation would provide a testing ground of the rotational diffusion model and would throw light on the role of intermolecular correlations. Recent experimental and simulation studies have revealed striking resemblance in orientational relaxation between the isotropic phase of thermotropic liquid crystals near the *I-N* transition and supercooled molecular liquids [27–33]. In view of this, the study of such a system would allow us to compare the behavior with what is typically observed in supercooled liquids.

Computer simulation using molecular models has proved to be useful to study orientational dynamics near the *I-N* transition. In a molecular dynamics simulation study with the Gay-Berne pair potential [34], de Miguel *et al.* found the ratio τ_1/τ_2 to be always less than 3 in the isotropic phase. They found that the departure from the Debye limit was pronounced when density was reduced or temperature was increased. Vasanthi *et al.* in extensive molecular dynamics simulations using the same model studied the aspect ratio dependence of the hydrodynamic prediction of translational-rotation coupling [35]. Recently Jose and Bagchi have tested the DSE relationship near the *I-N* phase transition in a system of the Gay-Berne ellipsoids of revolution [36]. They have shown that the DSE relation between the rotational friction and viscosity breaks down near the *I-N* phase transition.

In this work, we have investigated the rank dependence of orientational relaxation in a system of Gay-Berne ellipsoids of revolution near the *I-N* phase boundary in close connection with the Debye rotational diffusion model. The motivation of the present work comes partly from recent reports of the observed similarity in the orientational relaxation between thermotropic liquid crystals and supercooled molecular liquids [27–33]. We find that the ratio τ_1/τ_2 becomes much less than unity as the *I-N* phase boundary is

approached from the isotropic side. Simultaneously, the ratio τ_2/η becomes much larger than the hydrodynamic value near the *I-N* transition. We have also analyzed the breakdown of the Debye model of rotational diffusion in ratios of higher order orientational correlation times. We have provided a mode coupling theory analysis to explain the results. Theoretical analysis shows that the breakdown of the DSE model can be attributed to the growth of orientational pair correlation. Thus, the present analysis seems to suggest that one does not always need to invoke large scale jump diffusion to explain the decrease of the ratio τ_1/τ_2 from the Debye limit.

In the next section, we describe the system and simulation details. Results of our molecular dynamics simulation study of a system of ellipsoids of revolution with an aspect ratio equal to 3 along an isotherm and an isochore across the *I-N* phase transition are presented in Sec. III. These results show that the ratio τ_1/τ_2 can become much less than unity. This section also includes results for higher rank orientational time correlation functions. In Sec. IV, we present a theoretical analysis that can explain several aspects of these results. Section V provides a summary of our results and concluding remarks.

II. SYSTEM AND SIMULATION DETAILS

Here we consider a system of molecules with axial symmetry interacting with the Gay-Berne (GB) pair potential that has served as a standard model in the simulation studies of thermotropic liquid crystals. In the GB pair potential [37,38], each molecule is assumed to be an ellipsoid of revolution having a single-site representation in terms of the position $\mathbf{r}_i$ of its center of mass and a unit vector $\mathbf{e}_i$ along its principal axis of symmetry. The GB interaction between molecules i and j is given by

$$U_{ij}^{GB}(\mathbf{r}_{ij},\mathbf{e}_i,\mathbf{e}_j)=4\epsilon(\hat{\mathbf{r}}_{ij},\mathbf{e}_i,\mathbf{e}_j)(\rho_{ij}^{-12}-\rho_{ij}^{-6}), \quad (4)$$

where

$$\rho_{ij}=\frac{r_{ij}-\sigma(\hat{\mathbf{r}}_{ij},\mathbf{e}_i,\mathbf{e}_j)+\sigma_0}{\sigma_0}. \quad (5)$$

Here σ_0 defines the cross-sectional diameter, r_{ij} is the distance between the centers of mass of molecules i and j, and $\hat{\mathbf{r}}_{ij}=\mathbf{r}_{ij}/r_{ij}$ is a unit vector along the intermolecular separation vector $\mathbf{r}_{ij}$. The molecular shape parameter σ and the energy parameter ϵ both depend on the unit vectors $\mathbf{e}_i$ and $\mathbf{e}_j$ as well as on $\hat{\mathbf{r}}_{ij}$ as given by the following set of equations:

$$\sigma(\hat{\mathbf{r}}_{ij},\mathbf{e}_i,\mathbf{e}_j)=\sigma_0\left[1-\frac{\chi}{2}\left\{\frac{(\mathbf{e}_i\cdot\hat{\mathbf{r}}_{ij}+\mathbf{e}_j\cdot\hat{\mathbf{r}}_{ij})^2}{1+\chi(\mathbf{e}_i\cdot\mathbf{e}_j)}\right.\right.$$
$$\left.\left.+\frac{(\mathbf{e}_i\cdot\hat{\mathbf{r}}_{ij}-\mathbf{e}_j\cdot\hat{\mathbf{r}}_{ij})^2}{1-\chi(\mathbf{e}_i\cdot\mathbf{e}_j)}\right\}\right]^{-1/2} \quad (6)$$

with $\chi=(\kappa^2-1)/(\kappa^2+1)$ and

$$\epsilon(\hat{\mathbf{r}}_{ij},\mathbf{e}_i,\mathbf{e}_j)=\epsilon_0[\epsilon_1(\mathbf{e}_i,\mathbf{e}_j)]^\nu[\epsilon_2(\hat{\mathbf{r}}_{ij},\mathbf{e}_i,\mathbf{e}_j)]^\mu, \quad (7)$$

where the exponents μ and ν are adjustable, and

$$\epsilon_1(\mathbf{e}_i,\mathbf{e}_j)=[1-\chi^2(\mathbf{e}_i\cdot\mathbf{e}_j)^2]^{-1/2} \quad (8)$$

and
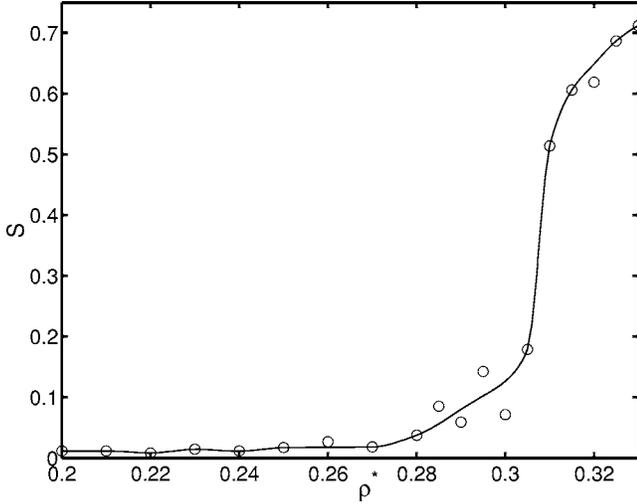
FIG. 1. The evolution of the orientational order parameter with density along the isotherm at temperature $T^\star = 1$.

$$\epsilon_2(\hat{\mathbf{r}}_{ij}, \mathbf{e}_i, \mathbf{e}_j) = 1 - \frac{\chi'}{2}\left[\frac{(\mathbf{e}_i \cdot \hat{\mathbf{r}}_{ij} + \mathbf{e}_j \cdot \hat{\mathbf{r}}_{ij})^2}{1 + \chi'(\mathbf{e}_i \cdot \mathbf{e}_j)} + \frac{(\mathbf{e}_i \cdot \hat{\mathbf{r}}_{ij} - \mathbf{e}_j \cdot \hat{\mathbf{r}}_{ij})^2}{1 - \chi'(\mathbf{e}_i \cdot \mathbf{e}_j)}\right]$$

(9)

with $\chi' = (\kappa'^{1/\mu} - 1)/(\kappa'^{1/\mu} + 1)$. Here $\kappa = \sigma_{ee}/\sigma_{ss}$ is the aspect ratio of the molecule with σ_{ee} denoting the molecular length along the major axis and $\sigma_{ss} = \sigma_0$, and $\kappa' = \epsilon_{ss}/\epsilon_{ee}$, where ϵ_{ss} and ϵ_{ee} are the depth of the minima of potential for a pair of molecules aligned parallel in a side-by-side configuration and end-to-end configuration, respectively. It follows that the GB pair potential defines a family of potential models, each member of which is characterized by a set of four parameters $(\kappa, \kappa', \mu, \nu)$. In the present work, we employ the Gay-Berne pair potential with the original and most studied parametrization $(3, 5, 2, 1)$ [39].

All quantities are given in reduced units defined in terms of the Gay-Berne potential parameters ϵ_0 and σ_0: length in units of σ_0, temperature in units of ϵ_0/k_B, and time in units of $(m\sigma_0^2/\epsilon_0)^{1/2}$, m being the mass of the ellipsoids of revolution. We set the mass as well as the moment of inertia of the ellipsoids equal to unity. The simulation is run in a microcanonical ensemble with the system in a cubic box with periodic boundary conditions. Further details of the simulation can be found elsewhere [31].

The system of Gay-Berne ellipsoids of revolution with aspect ratio 3 has been studied separately along an isotherm with density variation and along an isochore with temperature variation across the *I-N* transition. As compared to the density driven transition, the temperature driven *I-N* transition in the present system is known to be rather diffuse [39]. Next we present the results of our study.

III. RESULTS

A. Density variation along an isotherm

In Fig. 1, we show the orientational order parameter variation with density as a system of 576 Gay-Berne ellipsoids of revolution transits across the *I-N* transition along an
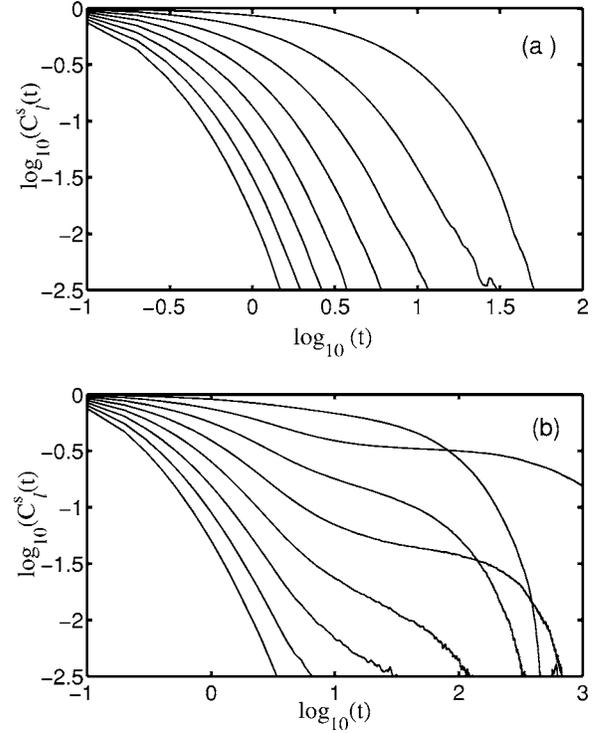
FIG. 2. The time evolution of the single-particle orientational time correlation functions, whose ranks range from 1 to 8, shown in a log-log plot at two densities corresponding to (a) $\rho^* = 0.285$; (b) $\rho^* = 0.315$. The curves are arranged in the decreasing order of ranks from the bottom to the top near the vertical axis in each plot.

isotherm at temperature $T^* = 1$. The phase transition is found to occur over a range of densities between 0.305 and 0.315. In Figs. 2(a) and 2(b), we show the decay of the single-particle OTCFs for the first eight ranks in the isotropic phase and near the *I-N* phase boundary, respectively. The *l*th rank single-particle OTCF is defined as

$$C_l^s(t) = \frac{\sum_i P_l[\hat{e}_i(0) \cdot \hat{e}_i(t)]}{\sum_i P_l[\hat{e}_i(0) \cdot \hat{e}_i(0)]},$$

(10)

where $\hat{e}_i(0)$ is the unit vector along the symmetry axis of the *i*th ellipsoid of revolution. The Debye model is found to hold good for all ranks of the single-particle OTCFs shown in Fig. 2(a) in the isotropic phase. As the rank of the correlation function increases, the relaxation time decreases.

Near the *I-N* phase boundary, as shown in Fig. 2(b), the relaxation of the single-particle OTCFs slows down considerably for all ranks. However, $C_l^s(t)$ is affected differently for different l values. The even and the odd *l*th OTCFs behave differently with the appearance of a pronounced plateau in $C_2^s(t)$ and $C_4^s(t)$. Such emergence of plateau is akin to what is observed for OTCFs in supercooled liquids at low temperatures [18,22].

Figure 2(b) shows that although the initial decay of $C_2^s(t)$ and $C_4^s(t)$ is faster than that of $C_1^s(t)$ and $C_3^s(t)$, respectively, the decay becomes slower at longer times. The even *l*th cor-
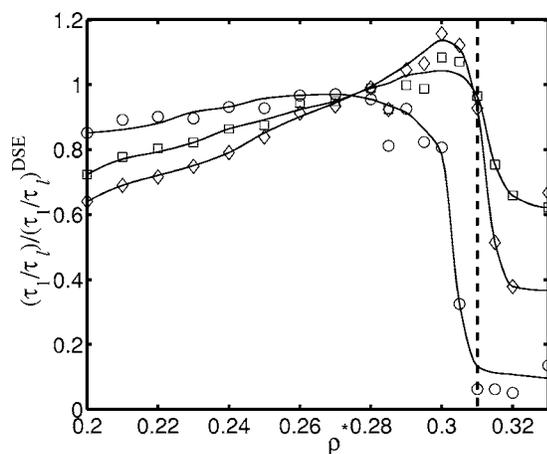
FIG. 3. The density variation of the ratios between the first-rank orientational correlation time and the second, third, and fourth rank orientational correlation times across the *I-N* transition. The circles represent the data for τ_1/τ_2, the diamonds for τ_1/τ_3, and the triangles for τ_1/τ_4. The ratios are scaled by the corresponding Debye predictions. The dashed vertical line marks the position of the *I-N* transition.

FIG. 5. The semilog plot of the ratio τ_l/η versus density for different l values. The circles show τ_l/η for $l=1$, the diamonds for $l=2$, the squares for $l=3$, and the triangles for $l=4$. The filled symbols show the ratios for even values of l.

relation functions both develop a rather long and distinct plateau. The decay of $C_4^s(t)$ is particularly revealing because it shows all the four phases of decay—the initial Gaussian, followed by the exponential, then the crossover to the plateau and the final exponential decay.

In Fig. 3, we show the evolution of the ratios τ_1/τ_2, τ_1/τ_3, and τ_1/τ_4 as increase in density drives the system across the *I-N* transition. Note that away from the *I-N* phase boundary in the isotropic phase, the ratios remain close to what are predicted by the Debye rotational diffusion model. However, as the *I-N* phase boundary is approached from the isotropic side, it is evident that the Debye rotational diffusion model breaks down completely.

In Fig. 4, we show the ratios between the second rank orientational correlation time and the higher rank ($l=3,4$) orientational correlation times as a function of density across

FIG. 4. The ratios between the second-rank orientational correlation time and the higher rank orientational correlation times across the *I-N* transition. The triangles represent the data for τ_2/τ_3 and the circles for τ_2/τ_4. The ratios are scaled by the corresponding Debye predictions. Again the dashed vertical line marks the position of the *I-N* transition.

the *I-N* transition. Note that the *I-N* transition affects the second rank OTCF most due to the up-down symmetry of the molecular model studied in the present work. Figure 4 shows a cusplike behavior which is well known in the study of equilibrium critical phenomena of finite sized systems. Its appearance in dynamics suggests the existence of large scale fluctuations in the orientational order parameter [40]. Since the second rank orientational time correlation function is associated with the optical response of the system, which undergoes dramatic increase near the *I-N* transition [40,41], the most affected orientational memory function is the second-rank one.

Microscopically this phenomenon may be understood qualitatively in terms of the molecular field theory of Maier and Saupe [40–42], where the molecule is confined in an effective field created by its neighbors. This effective potential is given by the expression

$$u_i = -\frac{A}{V^2}\frac{1}{2}S[3\cos^2(\theta_i)-1], \qquad (11)$$

where A is constant independent of the temperature, volume, and pressure, V is the molecular volume, and θ_i is the angle between molecular axis with a preferred axis. This effective potential grows as the order parameter increases. Note that a π rotation of the molecular axis relaxes $C_1^s(t)$ but not $C_2^s(t)$. This effect is manifested in the higher order OTCFs also. However, a random orientation of the smaller angle less than $\pi/2$ is only required for the relaxation of the $C_l^s(t)$ with $l \geqslant 3,4,\ldots$, etc. Hence the slow down of relaxation at these ranks appears as S becomes significantly large. In Sec. IV, we present a quantitative theory to describe these effects.

Another important aspect of the DSE which has been a subject of intense study in the literature of supercooled liquids is the viscosity (η) dependence of the time constants (τ_l) of OTCFs. In Fig. 5, we present the semilog plot of this ratio against density. The ratio remains a constant in the isotropic
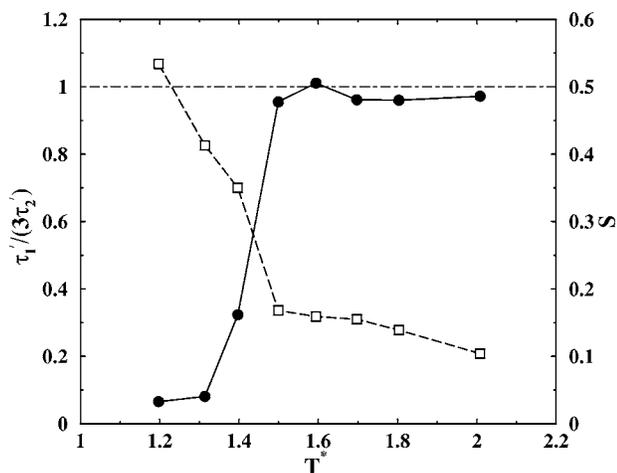
FIG. 6. The evolution of the ratio between the first-rank and the second-rank orientational correlation times with temperature across the I-N transition (circles). The inclusion of the scaling factor ensures that the ratio is equal to unity in the Debye limit as shown by the dot-dashed line. On a different scale shown on the right is the orientational order parameter variation with temperature (squares).

phase of the liquid crystals, in agreement with hydrodynamic prediction. This is also in accordance with the earlier simulation [36] which shows that the ratio between the rotational friction and the viscosity also shows similar behavior.

Note that unlike in supercooled liquids, the growth in the viscosity of the nematogens near the I-N transition is not rapid [36]. Therefore, the ratio between τ_l and η deviates from the DSE prediction largely due to the growth of τ_l. It is also evident that the violation of the DSE is found to be different for the odd and the even values of l. In Fig. 5, the ratios between τ_l and η for even l values grow more dramatically than that for odd l values.

B. Temperature variation along an isochore

In this work, we have also studied orientational relaxation in a system of 500 Gay-Berne ellipsoids of revolution with the use of the same parameterization but along an isochore at the density $\rho^\star = 0.32$. The drop in temperature drives the system from the isotropic to the nematic phase with the growth in the orientational order. In particular, the single-particle second-rank orientational correlation function decays with such a long time scale near the I-N phase boundary that an integral second-rank orientational correlation time is beyond the scope of the present simulation study. The poor data quality at long times with the present run length restricts us from having a reasonable fit of the long-time decay. In order to have an estimate of the second-rank orientational correlation time for the sake of comparison of the rank-dependent orientational correlation times, we define a correlation time $\tau_l'(T)$ that is the time taken for the single-particle lth rank OTCF to decay by 90% at a temperature T. The prime is used to distinguish it from the corresponding integral orientational correlation time.

Figure 6 shows that the ratio τ_1'/τ_2' follows the Debye behavior away from the I-N transition, but the onset of the

rapid growth of the orientational order parameter near the I-N transition induces a marked deviation from the Debye limit and the ratio falls rapidly. On the other hand, the ratios τ_1/τ_l go through maxima on transit from the isotropic phase to the nematic phase for both $l=3$ and $l=4$ as shown in Fig. 7, and the maxima correspond to the temperature below which the orientational order parameter is on the rapid rise. Figure 8 illustrates the temperature behavior of the ratios τ_2'/τ_l' across the I-N transition for $l=3$ and 4. While only a small deviation from the Debye behavior is apparent even at high temperatures away from the I-N transition, the onset of the growth of the orientational parameter marks a sharp increase in these ratios. The results, embodied in Figs. 6–8, suggest that orientational correlation, which builds up across the I-N transition, plays a key role in deviation from the Debye behavior of the orientational correlation times.

The contrast between the study along an isotherm and that along an isochore reveals the importance of the role played by the intermolecular potential in the breakdown of the DSE relation. In the study along the isotherm, the free volume that

FIG. 7. The temperature dependence of the ratio between the first rank and the lth rank orientational correlation times across the I-N transition for $l=3$ and 4. The inclusion of the scaling factor ensures that the ratio is equal to unity in the Debye limit as shown by the dot-dashed line.
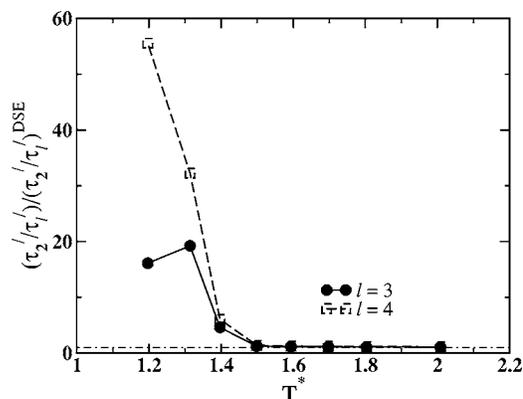
FIG. 8. The temperature dependence of the ratio between the second rank and the lth rank orientational correlation times across the I-N transition for $l=3$ and 4. The inclusion of the scaling factor ensures that the ratio is equal to unity in the Debye limit as shown by the dot-dashed line.

is available for the rotation reduces, thus leading to the formation of the orientational caging. In contrast, when temperature is reduced, the attractive part of the intermolecular potential becomes more dominant and results in the formation of the orientational caging that arrests the orientational random walk of the molecules. The above difference arises because temperature variation leads only to small changes in density because of the dominance of the repulsive part of the potential in determining the liquid structure.

IV. THEORETICAL ANALYSIS OF ORIENTATION RELAXATION

Here we present a mode coupling theory (MCT) analysis of the above relaxation behavior. MCT has a long and honorable history in describing dynamics near phase transitions [43–45]. Our starting point of the theoretical analysis is the Zwanzig-Mori continued fraction representation of the frequency dependent orientational time correlation function $C_l(z)$ [26,46–48]:

$$C_l^s(z) = \frac{1}{z + \dfrac{l(l+1)k_BT}{I[z + \Gamma_l(z)]}}, \tag{12}$$

where I is the moment of inertia and $\Gamma_l(z)$ is the Laplace frequency (z) and rank-dependent memory function. The latter is determined by the torque-torque correlation function. In general, it is very difficult to determine this correlation function from first principles, but as a first approximation, we would combine input from the mode coupling theory with that from the time-dependent density functional theory to obtain an expression for the memory function $\Gamma_l(z)$ which can be used to understand the reasons for the breakdown of the DSE model. Near the *I-N* transition the memory function $\Gamma(z)$ can be written as a sum of two parts

$$\Gamma_l(z) = \Gamma^{\text{bare}} + \Gamma_l^{\text{sing}}(z), \tag{13}$$

where the bare part of the memory function is assumed to be rank and frequency independent. This can be described by the two-body (binary) collision model. Note that in conjunction with Eq. (12), Γ^{bare} leads to the DSE behavior. The singular part of the memory function contains effects of intermolecular correlation and is rank dependent. It is given by [27,28,48]

$$\Gamma_l^{\text{sing}}(z) = \frac{3k_BT\rho}{8\pi^3I} \int_0^\infty dt e^{-zt} \int_0^\infty dk k^2 \sum_m c_{llm}^2(k) F_{lm}(k,t). \tag{14}$$

In the above equation, Γ_l is the rank and frequency dependent memory function. This is a function of the l,l,m component of the wave-vector-dependent direct correlation function $c_{llm}(k)$ (in the intermolecular frame). $F_{lm}(k,t)$ is the l,m component of the orientation dependent self-intermediate scattering function. The $F_{lm}(k,t)$ is defined in terms of the spherical harmonics as
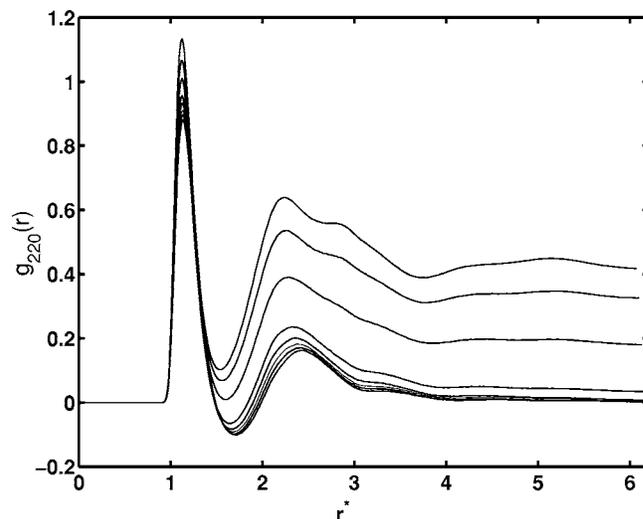
FIG. 9. The g_{220} component of the pair correlation function versus the pair separation at several densities across the *I-N* transition. The curves staring from the bottom to the top are corresponding to densities between $\rho^*=0.285$ and $\rho^*=0.315$ on a grid of $\delta\rho^* =0.005$.

$$F_{lm}(k,t) = \langle e^{\mathbf{k}\cdot[\mathbf{r(t)}-\mathbf{r(0)}]}Y_{lm}(\Omega,0)Y_{lm}(\Omega,t)\rangle. \tag{15}$$

The single particle position and orientation-dependent $\Gamma(\mathbf{r} -\mathbf{r}',t-t',\mathbf{\Omega},\mathbf{\Omega}')$ memory function is related to the torque-torque correlation function through the density functional theory by following the fluctuation dissipation theorem [46,48]. Note that $\Gamma_l^{\text{sing}}(z)$ contains the integration over the wave vector dependence. The slowdown of the relaxation of single particle OTCF is related to the nature of the component of the dynamics structure factor.

It is important to note that the rotational friction depends on the rank of the OTCF, and this friction differs from rank to rank because of vastly different wave vector dependence of $F_{\ell m}(k,t)$ for different ℓ particularly at low wave numbers. Near the *I-N* transition, due to existence of large wavelength fluctuations, the $k\to0$ component of the $F_{20}(k,t)$ undergoes a very slow decay and this is responsible for the slow down of the relaxation of $C_2^s(t)$. In this limit, the expression for $F_{lm}(k,t)$ is given by [46]

$$F_{lm}(k,t) = S_{lm}(k)e^{-l(l+1)D_Rt/S_{lm}(k)}, \tag{16}$$

where $S_{lm}(k)$ is the orientation dependent structure factor and D_R is the rotational diffusion coefficient. The $S_{lm}(k)$ is given by the expression

$$S_{lm}(k) = \langle e^{\mathbf{k}\cdot(\mathbf{r}-\mathbf{r}')}Y_{lm}(\Omega,0)Y_{lm}(\Omega',t)\rangle. \tag{17}$$

Near the *I-N* transition, $S_{20}(k)$ grows as $1/B^2k^2$, where

$$B^2 = \frac{\rho}{4\pi}\left(\frac{d^2c_{ll'm}(k)}{dk^2}\right)_{k=0}.$$

The growth of orientational pair correlation with the approach of the *I-N* transition is evident in Fig. 9. Note that starting from density $\rho^*=0.305$, the orientational pair corre-

lation function becomes nonzero even at large intermolecular separations. This is reflected in the rapid growth of $S_{20}(k)$ as $k \to 0$ near the *I-N* transition.

Combination of the above factors provides the following simple expression for the frequency dependence of the singular part of the memory kernel

$$\Gamma_2^{\text{sing}}(z) = A/\sqrt{z}, \tag{18}$$

where A is a numerical constant [27]. Note that such a power law dependence is absent from all odd ℓ th Γ_ℓ but in principle present in all the even ℓ. However, as ℓ increases, the decay becomes increasingly inertial and the role of intermolecular correlation becomes weak beyond $\ell = 4$. But for $\ell = 2$ and $\ell = 4$, the inverse square root dependence of the rotational memory function leads to a markedly slower power law decay as seen from Fig. 2(b).

Physically, this power law is a manifestation of the growth of the pseudonematic domains near the *I-N* phase boundary. A particle inside this domain feels a localizing potential that makes its rotation difficult. However, even within such a domain, a rotation of an individual particle by 180° (that is, by π) is possible because of the up-down symmetry of the particle. However, in contradiction to the conceptualization prevalent in supercooled liquid literature, here such a half-cycle rotation relaxes only the odd rank correlation functions, leaving the even ranked ones unchanged. In the MCT description, the influence of the localizing potential enters through the two-particle direct correlation function $[c_{\ell\ell m}(k)]$ and the static structure factor $S_{\ell m}(k)$. Just as in the Maier-Saupe theory, the present mean-field theory description can capture the rank dependence of the effective localizing potential. The above mode coupling theory analysis is by no means complete, but it provides a semi-quantitative explanation of the observed rank dependence of the orientational correlation time near the *I-N* transition, in terms of the rapid growth of equilibrium orientational pair correlation function.

V. CONCLUDING REMARKS

Let us first summarize the main results presented here. We study a system of Gay-Berne model mesogens along an isotherm and an isochore separately across its isotropic-nematic phase transition to investigate the rank dependent single-particle orientational relaxation from the perspective of the Debye behavior. Our results demonstrate that orientational correlation that starts growing near the *I-N* transition as it is approached from the isotropic side induces a marked deviation from the Debye behavior. We present a theoretical analysis of our results within the framework of the mode-coupling theory. This mode coupling theory analysis pro-

vides a semiquantitative explanation of the observed rank dependence of the orientational correlation time near the *I-N* transition. This explanation does not invoke the existence of any large scale angular jump motion that randomizes and thereby leads to the decay of correlation of all ranks with the same rate. Instead, our analysis attributes the non-Debye rank dependence to the rapid growth of equilibrium orientational pair correlation function.

It is interesting to contrast the breakdown of the DSE relationship observed in the present study with what is found in supercooled molecular liquids. As already mentioned, in the supercooled liquids the DSE relationship is often discussed in the context of translation-rotation decoupling in the sense that the translational diffusion gets decoupled from the shear viscosity in deeply supercooled regime while the rotational diffusion remains coupled to it. In the cases where the DSE relationship has been found to break down, τ_l fails to track the rapid growth in shear viscosity resulting in a fall of the ratio τ_l/η [22]. The fall is more pronounced for τ_1 than τ_2, which can be attributed to the fact that the advent of the jump motion at low temperatures affects τ_1 more. In contrast, there is no signature of decoupling of the translational diffusion from the shear viscosity as the *I-N* transition is approached from the isotropic side. Instead, the rotational diffusion slows down considerably. This is understandable on the basis of the rapid growth of orientational pair correlation in the vicinity of the *I-N* transition. No such growth occurs in the spatial correlation. Thus, stress-stress time correlation function decays rapidly to zero even near the *I-N* phase boundary and no particular growth is observed in shear viscosity. Translational diffusion also does not suffer from any substantial fall even though anisotropy sets in with facile translation diffusion parallel to the director as compared to the one perpendicular to it [35]. However, the intriguing aspect is that it is τ_2 that is more affected in the vicinity of the *I-N* transition than τ_1. In general, the even rank OTCFs get affected more by the growth of orientational correlation than the preceding odd ranked functions.

In view of the results presented here, a comparative study between dielectric relaxation (which essentially measures the $\ell = 1$ OTCF) and light scattering or fluorescence depolarization or NMR experiments (all of these measure the $\ell = 2$ OTCF) would be a worthwhile exercise. In fact, a detailed theoretical analysis of dielectric relaxation near the *I-N* phase boundary seems to be lacking.

[1] P. Debye, *Polar Molecules* (Dover, New York, 1929).

[2] B. J. Berne and R. Pecora, *Dynamic Light Scattering* (Dover, New York, 1976).

[3] S. Cannistraro and F. Sacchetti, Phys. Rev. A **33**, 745 (1976).

[4] D. M. Heyes, M. J. Nuevo, J. J. Morales, and A. C. Branka, J. Phys.: Condens. Matter **10**, 10159 (1998).

[5] R. S. Moog, M. D. Ediger, S. G. Boxar, and M. D. Fayer, J. Phys. Chem. **86**, 4694 (1982).

[6] D. A. Pinnow, S. J. Candau, and T. A. Litovitz, J. Chem. Phys. **49**, 347 (1968).

[7] M. S. Beevers, J. Crossley, D. C. Garrington, and G. Williums, J. Chem. Soc., Faraday Trans. 2 **73**, 458 (1977).

[8] D. Kivelson and S. A. Kivelson, J. Chem. Phys. **90**, 4464 (1989).

[9] F. Fujara, B. Geil, H. Sillescu, and G. Fleischer, Z. Phys. B: Condens. Matter **88**, 195 (1992).

[10] I. Chang, F. Fujara, B. Geil, G. Heuberger, T. Mangel, and H. Sillescu, J. Non-Cryst. Solids **172-174**, 248 (1994).

[11] M. T. Cicerone, F. R. Blackburn, and M. D. Ediger, J. Chem. Phys. **102**, 471 (1995).

[12] M. T. Cicerone and M. D. Ediger, J. Chem. Phys. **104**, 7210 (1996).

[13] F. H. Stillinger and J. A. Hodgdon, Phys. Rev. E **50**, 2064 (1994); **53**, 2995 (1996).

[14] G. Tarjus and D. Kivelson, J. Chem. Phys. **103**, 3071 (1995).

[15] K. L. Ngai, J. Phys. Chem. B **103**, 10684 (1999).

[16] M. D. Ediger, Annu. Rev. Phys. Chem. **51**, 99 (2000).

[17] H. Sillescu, J. Non-Cryst. Solids **243**, 81 (1999).

[18] S. Kämmerer, W. Kob, and R. Schilling, Phys. Rev. E **56**, 5450 (1997).

[19] L. Andreozzi, A. Di Schino, M. Giordano, and D. Leporini, J. Phys.: Condens. Matter **8**, 9605 (1996); Europhys. Lett. **38**, 669 (1997).

[20] S. Corezzi, S. Capaccioli, G. Gallone, M. Lucchesi, and P. A. Rolla, J. Phys.: Condens. Matter **11**, 10297 (1999).

[21] S. H. Bielowka, T. Psurek, J. Ziolo, and M. Paluch, Phys. Rev. E **63**, 062301 (2001).

[22] C. De Michele and D. Leporini, Phys. Rev. E **63**, 036702 (2001).

[23] M. Faetti, M. Giordano, D. Leporini, and L. Pardi, Macromolecules **32**, 1876 (1999).

[24] L. Andreozzi, M. Giordano, and D. Leporini, J. Non-Cryst.

Solids **235-237**, 219 (1998).

[25] L. Andreozzi, F. Cianflone, C. Donati, and D. Leporini, J. Phys.: Condens. Matter **8**, 3795 (1996).

[26] S. Ravichandran and B. Bagchi, Int. Rev. Phys. Chem. **14**, 271 (1995).

[27] S. D. Gottke, D. D. Brace, H. Cang, B. Bagchi, and M. D. Fayer, J. Chem. Phys. **116**, 360 (2002).

[28] S. D. Gottke, H. Cang, B. Bagchi, and M. D. Fayer, J. Chem. Phys. **116**, 6339 (2002).

[29] H. Cang, J. Li, and M. D. Fayer, Chem. Phys. Lett. **366**, 82 (2002).

[30] H. Cang, J. Li, V. N. Novikov, and M. D. Fayer, J. Chem. Phys. **118**, 9303 (2003).

[31] P. P. Jose and B. Bagchi, J. Chem. Phys. **120**, 11256 (2004).

[32] P. P. Jose, D. Chakrabarti, and B. Bagchi, Phys. Rev. E **71**, 030701(R) (2005).

[33] D. Chakrabarti, P. P. Jose, S. Chakrabarty, and B. Bagchi, Phys. Rev. Lett. **95**, 197801 (2005).

[34] E. de Miguel, L. F. Rull, and K. E. Gubbins, Phys. Rev. A **45**, 3813 (1992).

[35] R. Vasanthi, S. Bhattacharyya, and B. Bagchi, J. Chem. Phys. **116**, 1092 (2001).

[36] P. P. Jose and B. Bagchi, J. Chem. Phys. **121**, 6978 (2004).

[37] B. J. Berne and P. Pechukas, J. Chem. Phys. **56**, 4213 (1972).

[38] J. G. Gay and B. J. Berne, J. Chem. Phys. **74**, 3316 (1981).

[39] E. de Miguel and C. Vega, J. Chem. Phys. **177**, 6313 (2005).

[40] P. G. de Gennes and J. Prost, *The Physics of Liquid Crystals* (Clarendon Press, Oxford, 1993).

[41] S. Chandrasekhar, *Liquid Crystals* (Cambridge University Press, Cambridge, 1977).

[42] M. J. Stephen and J. P. Straley, Rev. Mod. Phys. **46**, 617 (1974).

[43] S. K. Ma and G. F. Mazenko, Phys. Rev. B **11**, 4077 (1975).

[44] P. C. Hohenberg and B. I. Halperin, Rev. Mod. Phys. **49**, 435 (1977).

[45] B. Bagchi and S. Bhattacharyya, Adv. Chem. Phys. **116**, 67 (2001).

[46] B. Bagchi and A. Chandra, Adv. Chem. Phys. **80**, 1 (1991).

[47] J. B. Hubbard and P. G. Wolynes, J. Chem. Phys. **69**, 998 (1978).

[48] B. Bagchi, J. Mol. Liq. **77**, 177 (1998).